BNL-223861-2023-TECH

EIC-ADD-TN-38

EIC Machine Protection System: safe operation of Rapid Cycling Synchrotron with updated parameters

S. Seletskiy

December 2022

Electron-Ion Collider Project

Brookhaven National Laboratory

U.S. Department of Energy

USDOE Office of Science (SC), Nuclear Physics (NP) (SC-26)

Notice: This technical note has been authored by employees of Brookhaven Science Associates, LLC under Contract No.DE-SC0012704 with the U.S. Department of Energy. The publisher by accepting the technical note for publication acknowledges that the United States Government retains a non-exclusive, paid-up, irrevocable, world-wide license to publish or reproduce the published form of this technical note, or allow others to do so, for United States Government purposes.

DISCLAIMER

This report was prepared as an account of work sponsored by an agency of the United States Government. Neither the United States Government nor any agency thereof, nor any of their employees, nor any of their contractors, subcontractors, or their employees, makes any warranty, express or implied, or assumes any legal liability or responsibility for the accuracy, completeness, or any third party's use or the results of such use of any information, apparatus, product, or process disclosed, or represents that its use would not infringe privately owned rights. Reference herein to any specific commercial product, process, or service by trade name, trademark, manufacturer, or otherwise, does not necessarily constitute or imply its endorsement, recommendation, or favoring by the United States Government or any agency thereof or its contractors or subcontractors. The views and opinions of authors expressed herein do not necessarily state or reflect those of the United States Government or any agency thereof.

EIC Machine Protection System: safe operation of Rapid Cycling Synchrotron with updated parameters

S. Seletskiy*

December 21, 2022

1 Introduction

This note considers safety of operation of the EIC Rapid Cycling Synchrotron (RCS) with updated RCS parameters (see Table 1).

Table 1: RCS electron beam parameters

Top energy (K) [GeV]	5	10	18
Bunch Charge (Q_b) [nC]	28	28	12
Bunches/injection cycle (after merge) (N_b)		2	
Injection emittance (norm.) (ε_x, ε_y) [μm]		40, 40	
Extraction emittance (norm.) (ε_x, ε_y) [μm]	196, 18	391, 26	845, 70
Minimum β_x, β_y [m]		1.7, 1.6	
Repetition rate f [Hz]		1	

Initial considerations related to the RCS Machine Protection System (MPS) can be found in [1]. The most recent RCS parameters are obtained from [2, 3].

This note is concerned only with a potential damage of in-vacuum components due to a direct beam deposit. The problem of the heating produced by the synchrotron radiation of the electron beam is not the topic of this note and is discussed in [4] (see Section 6.4.2 in [4] for relevant considerations).

*seletskiy@bnl.gov

2 Direct hit scenarios

Below we will consider two scenarios of electron beam directly hitting an in-vacuum surface.

First, we will consider what happens when the beam is deposited on a stainless steel or a copper surface at a normal incident angle. Such a failure is possible if a vacuum valve gets closed by an error. Depending on design details of the RCS, it can also happen if the beam is missteered to a crotch of a Y-shaped copper vacuum chamber.

The second scenario is when the beam hits a vacuum chamber at some grazing angle.

Finally, we will discuss the distributed partial losses due to halo scraping.

In the following calculations we assume thickness of in-vacuum components to be $w = 1$ mm [5], and we assume the same maximum grazing angle (θ), which was used in [1].

The total stopping power (E_{st}) and the collision stopping power (E_{col}) for the calculations are obtained from [6]. The respective plots based on provided stainless still composition (and for copper) and extrapolated to 18 GeV are shown in Figs. 1 and 2.

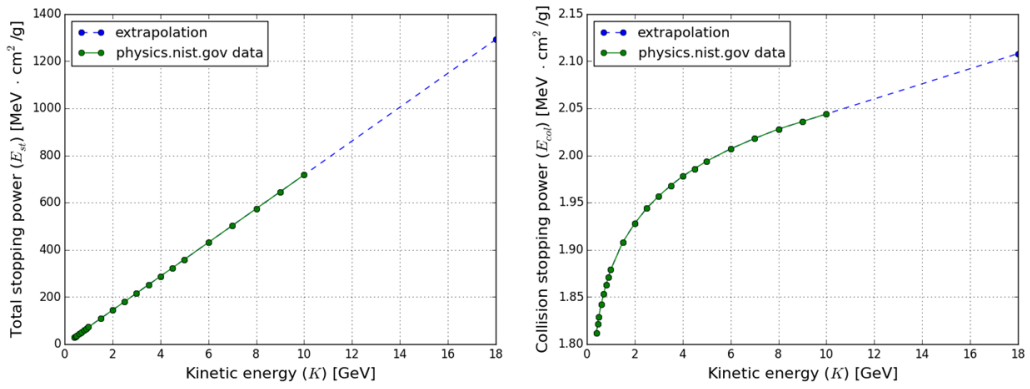


Figure 1: Stainless steel total and collision stopping power for electrons.

Table 2 shows parameters, which we use in the following calculations.

2.1 Direct hit at normal incident angle

In case of a normal incident angle the thermal energy loss per electron (per hit) is given by:

$$H = E_{col}\rho w \tag{1}$$

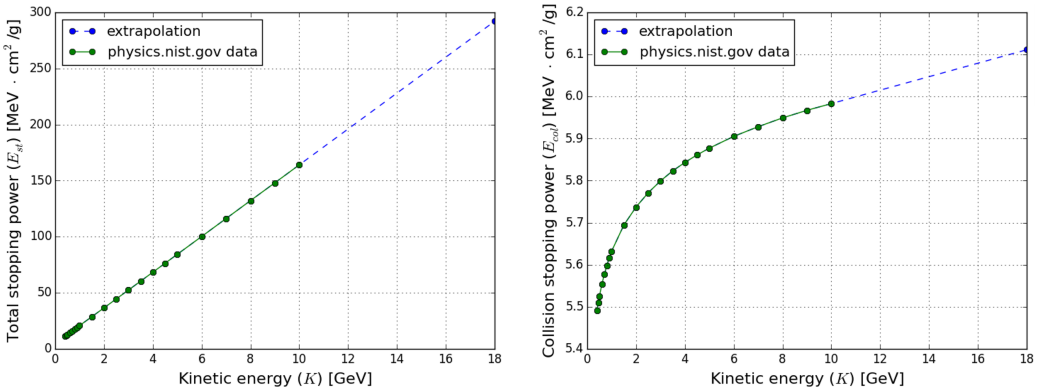


Figure 2: Copper total and collision stopping power for electrons.

Table 2: Parameters for direct hit calculations

Electron kinetic energy (K) [GeV]	5	10	18
Material thickness (w) [mm]		1	
Maximum grazing angle (θ) [mrad]		10	
		Stainless Steel	
Total stopping power (E_{st}) [MeV·cm^2/g]	359	718	1292
Collision stopping power (E_{col}) [MeV·cm^2/g]	1.99	2.04	2.11
		Copper	
Total stopping power (E_{st}) [MeV·cm^2/g]	78	158	292
Collision stopping power (E_{col}) [MeV·cm^2/g]	5.88	5.98	6.11

where the density of stainless steel is $\rho = 7999.5$ kg/m^3 and for copper $\rho = 8960$ kg/m^3.

The relative energy that an electron looses on a single hit is given by:

$$\delta_K = \frac{E_{st}\rho w}{K} \tag{2}$$

Figures 3 and 4 show H and δ_K for the full range of RCS parameters. Since, for stainless steel $\delta_K \cdot 100 \approx 6\%$, we conclude that the electrons will be lost inside the ring after a single hit (if a beam hits a Y-shaped copper vacuum chamber, then the beam is lost). Hence, the total heat load on the surface intercepting the e-beam can be calculated as:

$$H_{tot}[\mathrm{J}] = N_b Q_b[\mathrm{C}] H[\mathrm{eV}] \tag{3}$$

where N_b is the number of bunches in the RCS and Q_b is a bunch charge.

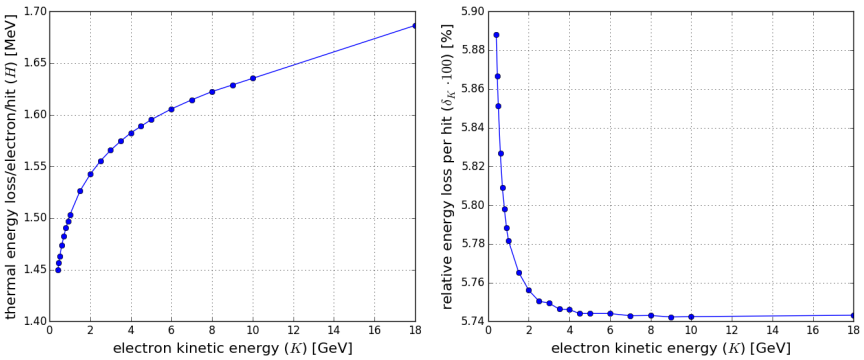


Figure 3: Stainless Steel: energy loss per electron for a hit at a normal incident angle.

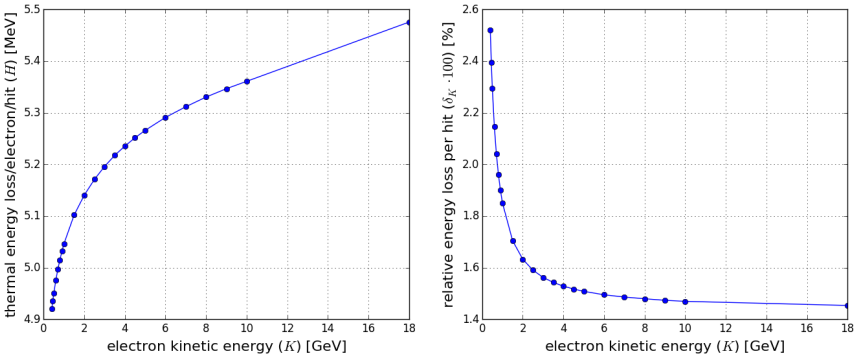


Figure 4: Copper: energy loss per electron for a hit at a normal incident angle.

The minimum rms size of the intercepted beam is $\sigma_{x,y} = \sqrt{\varepsilon_{x,y}\beta_{x,y}/\gamma}$, where $\beta_{x,y}$ are minimum β-functions in the RCS and $\varepsilon_{x,y}$ are normalized emittances. It is reasonable to use "injection emittances" for our calculations, because the final emittance blow-up is supposed to be preformed at top energy, right before the extraction. An area of a uniform distribution having the same density as a peak density of the Gaussian distribution with $\sigma_{x,y}$ is $A = 2\pi\sigma_x\sigma_y$. Therefore, a maximum instantaneous temperature increase of the hot-spot hit by the beam can be estimated as:

$$\Delta T = \frac{H_{tot}}{SHC \cdot \rho \cdot w \cdot 2\pi\sigma_x\sigma_y} = \frac{N_b Q_b E_{col}\gamma}{2\pi \cdot SHC \cdot \sqrt{\varepsilon_x\beta_x\varepsilon_y\beta_y}} \tag{4}$$

Here, a specific heat capacity for stainless steel is $SHC = 502.4$ [J/(kg·K)]

and for copper $SHC = 385$ [J/(kg·K)] .

Substituting parameters listed in Tables 1 and 2 into Eqs. (2)-(4) we get the instantenious temperature increase listed in Table 3 (see Section 4).

2.2 Direct hit at grazing angle

Let us consider the e-beam with the minimum β-functions hitting a vacuum chamber at a grazing angle $\theta = 10$ mrad (see [1] for details). The thickness of the material intercepting the e-bunch is:

$$D = w/\theta = 200 \text{ mm} \tag{5}$$

On the other hand, the distance that an electron with a kinetic energy K travels through the material until it is completely stopped is given by:

$$d = \frac{K}{E_{st}\rho} \tag{6}$$

Figure 5 shows that both for copper and for stainless steel $dl D$ for the whole range of energies of interest.

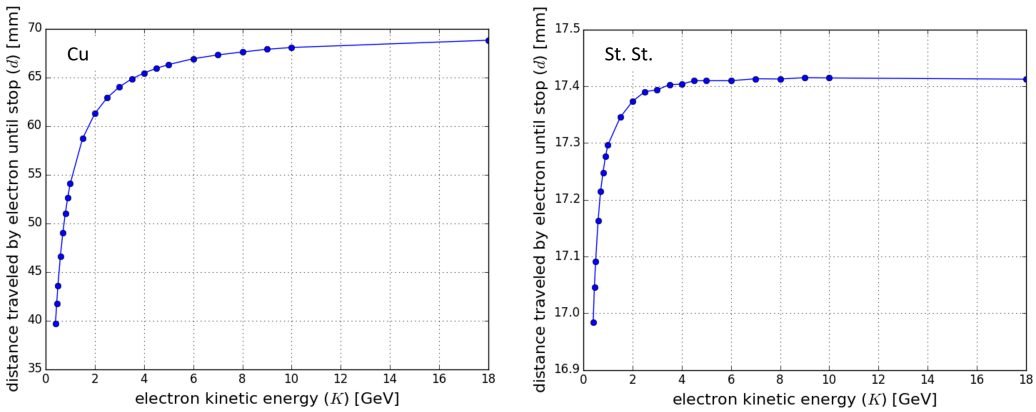


Figure 5: Distance traveled by an electron in the material of the vacuum chamber wall until the electron is fully stopped. The left plot is for copper and the right plot is for stainless steel.

Therefore, the distance d defines the thermal energy loss per electron for the direct hit at a grazing angle:

$$H_1 = E_{col}\rho d = K\frac{E_{col}}{E_{st}} \tag{7}$$

Figure 6 shows the result of (7) calculations.

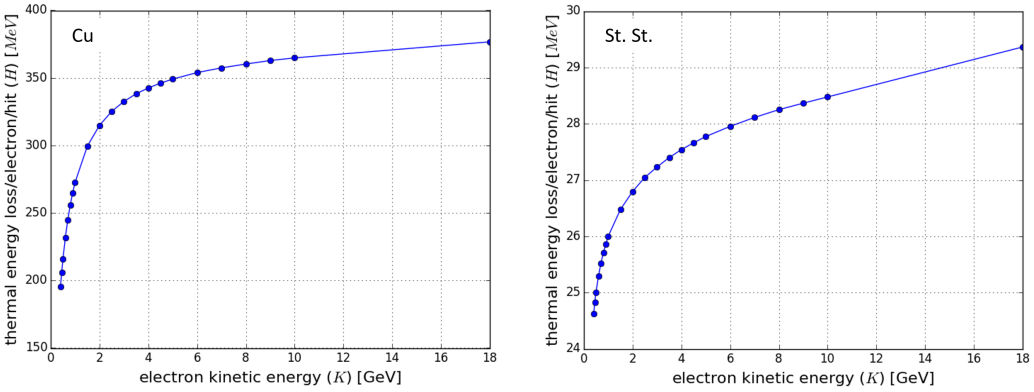


Figure 6: Energy loss per electron for a hit at a grazing angle. The left plot is for copper and the right plot is for stainless steel.

Next, similar to Eqs. (3) and (4) we get:

$$H_{tot1}[\mathrm{J}] = N_b Q_b[\mathrm{C}] H_1[\mathrm{eV}] = N_b Q_b[\mathrm{C}] K[\mathrm{eV}] \frac{E_{col}}{E_{st}} \tag{8}$$

$$\Delta T_1 = \frac{H_{tot1}\theta}{SHC \cdot \rho \cdot d \cdot 2\pi\sigma_x\sigma_y} = \frac{N_b Q_b E_{col}\gamma\theta}{2\pi \cdot SHC \cdot E_{st} \cdot \rho \cdot d \cdot \sqrt{\varepsilon_x\beta_x\varepsilon_y\beta_y}} K \tag{9}$$

Here we assumed that the area of the hot spot on the vacuum chamber is $A = 2\pi\sigma_x\sigma_y/\theta$.

Substituting beam parameters into Eq. (9) we get instantaneous temperature increases listed in Table 3. Notice, that since the vacuum chamber is made of copper, we show only the results for electrons heating copper surface at a grazing angle.

3 Partial losses

The maximum average power running through the RCS in a form of electron beam is:

$$P_{max} = K[\mathrm{GeV}] \cdot N_b \cdot Q_b[\mathrm{nC}] \cdot f[\mathrm{Hz}] = 10 \cdot 2 \cdot 28 \cdot 1 = 560[\mathrm{W}] \tag{10}$$

Even if 10% of this power is constantly lost due to halo scraping, it shouldn't cause an overheating problem.

A measurement of charge loss between an injection and an extraction to the level of a few percent can be realized either with two dedicated current

transformers or via comparison of sum signals from buttons of two BPMs (with proper BPM-to-BPM calibration).

To make operation safer one might consider installing thermocouples at locations of potential scraping (with large β-functions and/or a reduced vacuum chamber ID).

4 Results and conclusions

Results of the studies are summarized in Table 3. Notice, that the results are equally applicable to both the RCS itself and the RCS injection and extraction lines.

Table 3: Temperature increase of an in-vacuum surface directly hit by the e-beam

Electron kinetic energy (K) [GeV]	5	10	18
St. St. @ normal incident angle (ΔT) [K]	525	1076	856
Cu @ normal incident angle (ΔT) [K]	2018	4109	3237
Cu @ grazing angle $\theta = 10$ mrad (ΔT_1) [K]	20	41	32

An instantaneous temperature increase for a direct hit at a normal incident angle is in the range of $525 - 1076$ K for the stainless steel and in the range of $2018 - 3237$ K for the copper surface. While for stainless steel such an increase is less than the material melting temperature of 1450 C, it is large enough to cause an immediate mechanical damage to an in-vacuum component of the RCS. For copper the increase is higher than the melting temperature of 1084 C. Therefore, the beam must be aborted as soon as the conditions for a "90^o angle hit" failure are detected by the MPS.

A temperature increase for a direct hit at a maximum grazing angle of 10 mrad is less than or equal to 41 K. We can assume (see [1] for the details) that such an increase is safe.

Distributed losses due to halo scraping are not of particular concern. Nonetheless, we suggest interrupting the injection-extraction cycle if 1 nC loss of beam charge in "the injection beamline + the RCS + the extraction beamline" is detected.

We conclude that, from the "direct hit" point of view, the RCS MPS must satisfy the following criteria:

- To avoid a direct hit of an in-vacuum component by the electron beam at a normal incident angle the beam position monitors (BPMs) and

the in/out statuses of all the insertable devices (such as vacuum valves and profile monitors) must be included into the MPS.

- The BPMs' limits must be set in such a way that a local angular deflection of the beam orbit is guaranteed to be less than 10 mrad.
- The MPS requires an abort system. The abort time is defined by how fast the RCS insertable devices can reach the local e-beam orbit.
- If an abort system can be constructed in such a way that it deposits the e-beam on a vacuum chamber at an angle less than 10 mrad, then a dedicated dump line is not needed for the RCS.
- The operations must be interrupted upon detection of 1 nC loss per injection-extraction cycle.

We suggest the following MPS diagnostics for the RCS (including the RCS injection and extraction beamlines):

- BPMs,
- Insertable devices' limit switches,
- Two current transformers (at the injection line entrance and the extraction line exit),
- Thermocouples installed at the potential scraping locations.

References

[1] S. Seletskiy et al., Electron Ion Collider Machine Protection System: on the necessity of the MPS abort system for Rapid Cycling Synchrotron, BNL-222326-2021-TECH (2020).

[2] J. Rochford, Master Parameter Tables for the EIC, EIC-SEG-RSI-005 (September 14, 2022).

[3] Private communications with Dr. V. Ranjbar.

[4] F. Willeke et al., Electron Ion Collider Conceptual Design Report 2021, BNL-221006-2021-FORE, (2021).

[5] Private communications with D. Gassner and C. Hetzel.

[6] NIST Stopping power and range tables for electrons, `https://physics.nist.gov/PhysRefData/Star/Text/ESTAR.html`